Synthesis, structure, photophysics, and singlet oxygen sensitization by a platinum(II) complex of *meso*-tetra-acenaphthyl porphyrin

Antara Garai,[a] Marco Villa,[b] Marianna Marchini, [b] Sajal Kumar Patra,[a] Tanmoy Pain, [a] Sruti Mondal, [a] Paola Ceroni*[b] and Sanjib Kar*[a]

[a] *Dr. A. Garai, S. K. Patra, T. Pain, S. Mondal, Dr. S. Kar*
School of Chemical Sciences, National Institute of Science Education and Research (NISER), Bhubaneswar – 752050, India, and Homi Bhabha National Institute, Training School Complex, Anushakti Nagar, Mumbai, 400 094, India. E-mail: sanjib@niser.ac.in
http://www.niser.ac.in/~sanjib/

[b] *M. Villa, M. Marchini, Prof. Dr. P. Ceroni*
Department of Chemistry "G. Ciamician," University of Bologna, via Selmi 2, 40126 Bologna, Italy. E-mail: paola.ceroni@unibo.it
https://www.unibo.it/sitoweb/paola.ceroni

Abstract: A new platinum(II) porphyrin complex has been synthesized and characterized via various spectroscopic techniques. Single-crystal XRD analysis reveals that the geometry around the Pt(II) center is near the perfect square planar geometry. The Pt(II)-N bond distances are in the ranges of 2.005 Å─2.020 Å. The platinum(II) porphyrin derivative exhibited one reversible oxidative couple at +1.10 V and a reversible reductive couple at -1.47 V versus Ag/AgCl. In deaerated dichloromethane solution at 298 K, a strong phosphorescence is observed at 660 nm, with emission quantum yield of 35% and lifetime of 75 μs. Upon excitation of the acenaphthene chromophores at 300 nm, sensitised phosphorescence of the Pt(II) porphyrin is observed with a unitary efficient energy transfer, demonstrating that this system behaves as a light harvesting antenna. The red phosphorescence is strongly quenched by oxygen, resulting in singlet oxygen production with a very high quantum yield of 88%. This result indicates that this Pt(II) porphyrin is an excellent photosensitizer for the production of singlet oxygen and will have potential applications in the field of photodynamic therapy as well as oxygen sensors.

Introduction

Transition metal complexes have gained a lot of interest, thanks to their peculiar photophysical properties. Upon photoexcitation, transition metal complexes bearing heavy transition metals like ruthenium, iridium, gold, platinum, etc., show a very efficient intersystem crossing (ISC) thanks to the heavy atom effect and produce a triplet excited state. [1-6] This triplet excited state decay back to the ground state by non-radiative deactivation or by phosphorescence, with the emission of a photon. The long triplet lifetimes of these complexes (in the order of microseconds) are exploited for various energy transfer/electron transfer reactions. These photoactive transition metal complexes constitute an important class of molecules known as the photosensitizer.[7-12] The energy transfer from these photosensitized molecules to the natural triplet oxygen generates singlet oxygen.[13] Photosensitized singlet oxygen generation is an emerging research area with versatile applications in organic synthesis of fine chemicals,[14] pollution controls,[15] and photodynamic therapy.[16-19] In this regard, Ru(II) polypyridyl complexes,[20] iridium(III),[21-22] gold(I) complexes,[23] and platinum(II) porphyrin complexes[24-28] are well known as the photosensitizer. Platinum porphyrin complexes show intense phosphorescence at room temperature due to high yields of population of the triplet state and high yield of emission quantum yield. [29-32] Platinum porphyrin complexes have been used to detect oxygen via phosphorescence quenching phenomena. [33-35] The ideal dye for luminescence O_2 sensing material must be a good triplet emitter with a lifetime suitable for the specific range of oxygen concentration to be detected. Due to those reasons, ruthenium bipyridine complexes and platinum porphyrin complexes are often used as luminescence oxygen sensing materials. [36-38] Although the lifetime of triplet emitters varies largely from ruthenium-based dyes to platinum-based dyes, it is not so easy to fine-tune their triplet-state lifetime as the various application needs a distinctive triplet-sate lifetime of the dye. To achieve that purpose, a suitable design of the ligand system is a prerequisite. Thus there is an intense research interest in newer varieties of dyes having distinctive triplet lifetime. Interestingly, the absorption and emission spectra of platinum(II) porphyrins are very characteristic.[39] These compounds exhibited a large molar absorption coefficient, a large Stokes shift of the emission band, and a high quantum yield of luminescence at room temperature.[40] Due to their intense phosphorescence, platinum(II) porphyrin complexes are well-known photosensitizers and have found applications as phosphorescent markers in immunology,[41] in solar energy conversion and storage, [42] as molecular conductors, [43] and in oxygen sensing devices.[44] Porphyrins having increased conjugation at the β positions, often

called π-extended porphyrins, have attracted significant attention as potential candidates for optoelectronic materials.[45] These compounds exhibited phosphorescence in the red-near infrared (NIR) region of the spectrum.[46] However, similar studies with the increased conjugation at the *meso*-phenyl ring have not been covered that much. One possible reason is that the steric interaction between the porphyrin β hydrogen and the *meso*-phenyl ring does not allow appreciable π overlap between them, and thus, there is no significant effect on the electronic structure of the porphyrin.[47] However, it has to be kept in mind that the proper choice of the substituent's (either *meso*- or β-) at the porphyrin periphery can enhance the rigidity of the resulting structure and this might result in an increase of the phosphorescence quantum yield by slowing down non-radiative decay processes of the lowest triplet excited state. It was also reported earlier that steric crowding could enhance the lifetime of the triplet state of porphyrinoids.[47] Herein, we present the synthesis of a new platinum(II) porphyrin complex: [5,10,15,20-tetra(5-acenaphthyl)porphinato] platinum(II), **PtTANP** bearing acenaphthyl groups at their *meso*-positions (Scheme 1). Acenaphthene, an aromatic hydrocarbon obtained from coal tar is derived via simple modification of naphthalene unit and has found extensive applications in dyes and drugs and is also biocompatible. [48] The compound **PtTANP** has been thoroughly characterized by several spectroscopic techniques, including UV-Vis, emission, ^{1}H and ^{13}C NMR, ESI-MS data, and single-crystal XRD analysis.

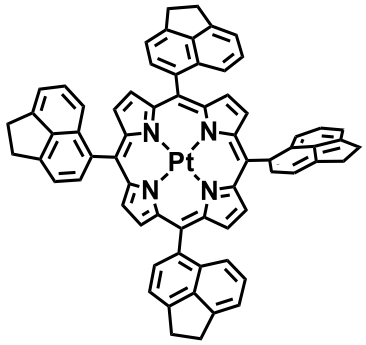

PtTANP

Scheme 1 Structure of the [5,10,15,20-tetra(5-acenaphthyl)porphinato] platinum(II), **PtTANP**.

RESULTS AND DISCUSSION

Synthesis and characterization

The reaction of the 5,10,15,20-tetra(5-acenaphthyl) porphyrin, **H_2TANP** with the platinum precursor complex K_2PtCl_4 in benzonitrile solution resulted in the formation of the complex, [5,10,15,20-tetra(5-acenaphthyl)porphinato] platinum(II), **PtTANP** (Scheme 2). The purity and identity of the platinum (II) complex, **PtTANP** is demonstrated by its satisfactory elemental analyses, ESI-MS data, NMR, UV-Vis, emission, and single-crystal XRD data (Figures S1-S5). The electrospray mass spectrum showed the peaks centered at *m/z* = 1112.3391 corresponding to [**PtTANP**+H]$^+$ (calculated molecular mass: 1112.3292) (Figure S3).

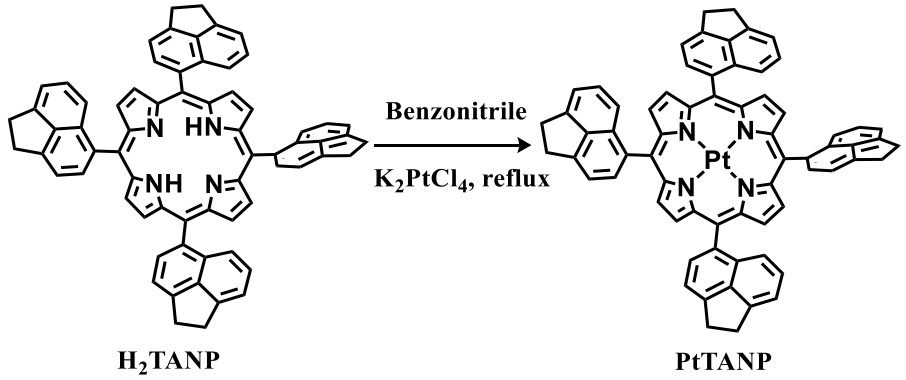

Scheme 2. Synthesis of [5,10,15,20-tetra(5-acenaphthyl)porphinato] platinum(II), **PtTANP**.

The ^{1}H NMR and ^{13}C NMR spectrum of **PtTANP** in $CDCl_3$ are shown in Figures S1-S2. The ^{1}H NMR spectrum of **PtTANP** exhibits the expected number of 44 partially overlapping protons in the region, δ=3.62–8.50 ppm (Figure S1). The methylene group protons resonate at 3.62-3.70 ppm (m, 16H) in $CDCl_3$. The 28 aromatic protons resonate at 6.81 - 8.50 ppm.

Crystal Structure

The crystal system of [5,10,15,20-tetra(5-acenaphthyl)porphyrinato] platinum(II), **PtTANP** is triclinic, and the unit cell has two molecules of **PtTANP**. Important crystallographic parameters for **PtTANP** are summarized in Table S1. Bond angles and distances of **PtTANP** match nicely with the previously reported other authentic porphyrinato platinum(II) derivatives. The deviation of the pyrrolic nitrogen atoms from the mean twenty carbon atom porphyrin plane by distances ranging from 0.008─ 0.049 Å in **PtTANP** (Figure

1). The observed deviations in **PtTANP** are in good agreement with that of the previously reported [5,10,15,20-tetra(5-acenaphthyl)porphyrinato] zinc(II) derivative.[49] However, the dihedral angles of the *meso*-substituted acenaphthyl rings and the 20-carbon mean porphyrin plane differs significantly in **PtTANP** in comparison with [5,10,15,20-tetra(5-acenaphthyl)porphyrinato] zinc(II). The corresponding values are of 65.68─75.20° in **PtTANP** and of 81.23─85.32° in [5,10,15,20-tetra(5-acenaphthyl)porphyrinato] zinc(II). While the deviation of Platinum atom from the mean N4 porphyrin plane is 0.0031 Å, the similar deviation in the case of the Zn(II) complex is zero. This can be ascribed to the smaller ionic radius of Zn(II). The geometry around the Pt (II) center is very near to the perfect square planar. The bite angles of N1-Pt-N2, N2-Pt-N3, N3-Pt-N4, and N4-Pt-N1 are 90.24°, 90.13°, 89.76°, and 89.87°, respectively. The Pt(II)-N bond distances are in the ranges of 2.005 Å─2.020 Å. These bond distances and angles match reasonably well with the previously reported authentic **PtTPP** derivatives (TPP=5,10,15,20-tetraphenyl-porphinato).[50] Similar bond distances were reported to be 2.08 Å in **PtTPP** derivatives.

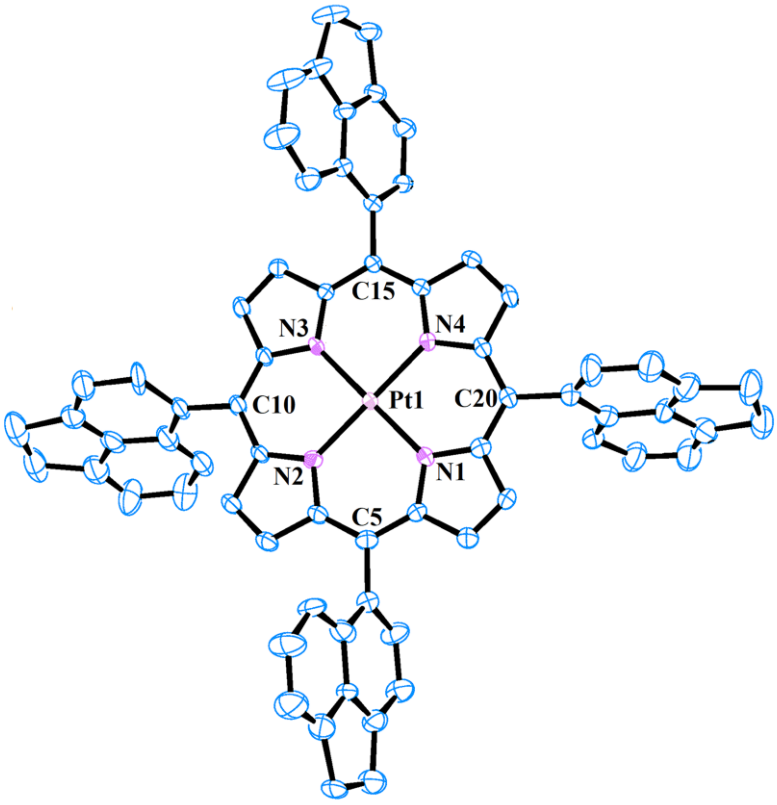

Figure 1 ORTEP diagram of **PtTANP**. Ellipsoids are drawn at 40% probability.

Electrochemistry

To understand the redox properties of **PtTANP**, the cyclic voltammetric and differential pulse voltammetric measurements were performed by using tetraethyl ammonium perchlorate (TEAP, 0.1 M) as a supporting electrolyte (Figure 2, Table S2) in dichloromethane solution.

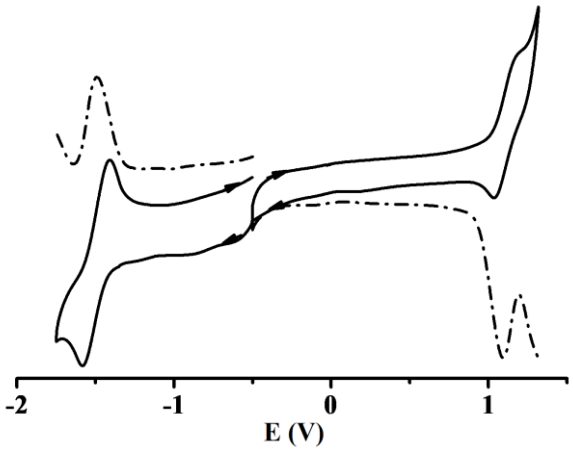

Figure 2 Cyclic voltammogram (black solid line) and differential pulse voltammogram (black doted line) of **PtTANP** in dichloromethane under a nitrogen atmosphere. The potentials are *vs.* Ag/AgCl.

Ag/AgCl reference electrode was used to express the potentials. The **PtTANP** derivative exhibited one reversible oxidation couple at +1.10 V (ΔE_p = 80 mV). It also showed one reversible reduction couple at -1.47 V (ΔE_p = 80 mV) versus Ag/AgCl. For a similar platinum porphyrin derivative, **PtTPP**, the 1st oxidation couple at +1.15V and the 1st reduction couple at -1.35V versus Ag/AgCl in dichloromethane, [51] demonstrating a slight negative shift of the reduction potential of **PtTANP** with respect to **PtTPP**.

Photophysical properties and Singlet oxygen sensitization

The photophysical characterization of the platinum porphyrin complex **PtTANP** was carried out in dichloromethane or toluene: since no significant difference was observed (Figure S5), the photophysical properties in dichloromethane will be discussed. The absorption spectrum (solid line in Figure 3) shows the typical Soret band at 410 nm with an absorption coefficient of 2.24 × 10^5 $M^{-1}cm^{-1}$ and the typical Q-bands with vibrational structure at 512 nm (ε = 3.0 × 10^4 $M^{-1}cm^{-1}$) and 542 nm (ε = 0.9 × 10^4 $M^{-1}cm^{-1}$). The additional band at 300 nm is due to the acenaphthene chromophores (ACN). [52a]

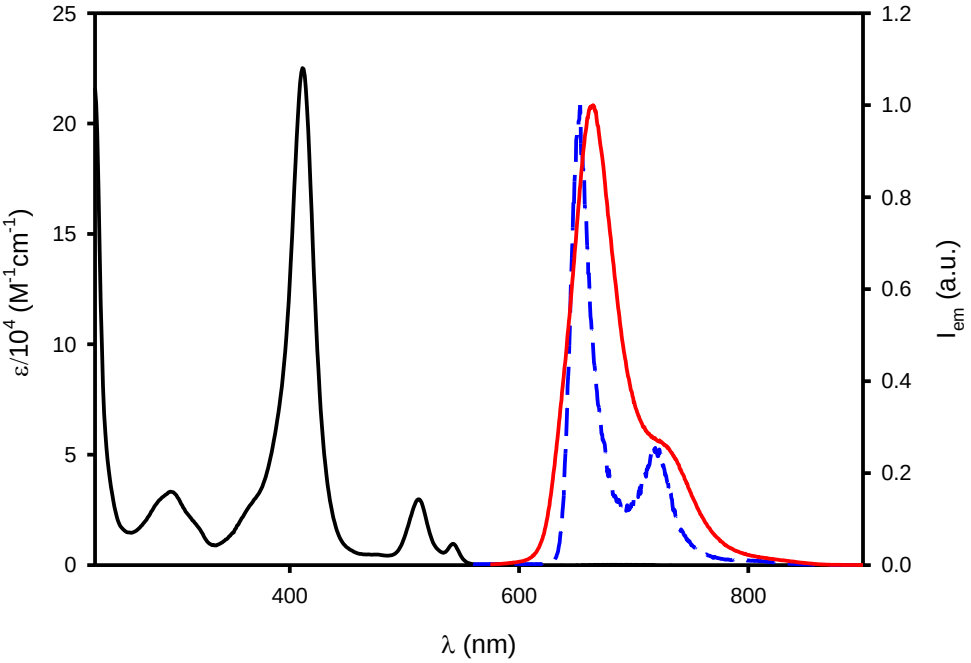

Figure 3 Absorption (black solid line) and emission spectra in deaerated (red solid line) dichloromethane solution of **PtTANP** (λ_{exc} =400 nm) at 298K. Emission spectrum in a rigid matrix of DCM-MeOH 1:1 at 77K (dashed blue line, λ_{exc} =400 nm).

In deaerated solution at 298 K, a strong phosphorescence is observed with maximum at 660 nm (red line in Figure 3), phosphorescence quantum yield of 35% and lifetime of 75 µs. The excitation spectrum performed at λ_{em} = 660 nm well matches the absorption spectrum (Figure S6), demonstrating a unitary efficient energy transfer from the acenaphthene chromophores to the Pt(II) porphyrin. Indeed, upon excitation at 300 nm, where most of the light is absorbed by acenaphthene chromophores, sensitised emission at 660 nm is observed. Therefore, **PtTANP** behaves as a light harvesting antenna as schematically depicted in Figure 4.

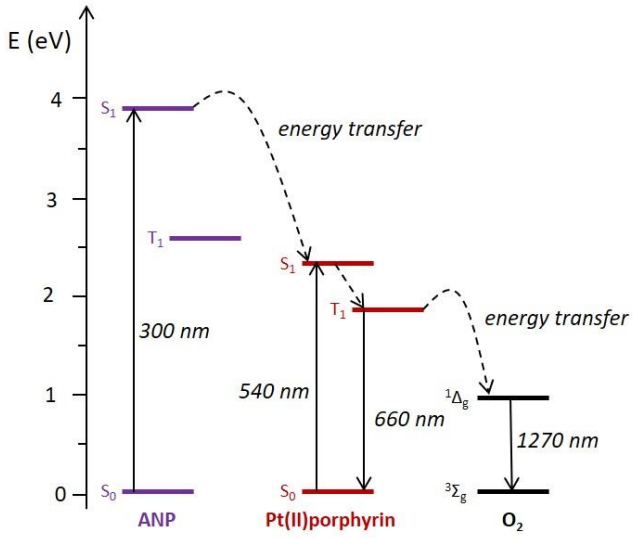

Figure 4 Most relevant photophysical processes occurring for **PtTANP**, constituted by a Pt(II) porphyrin core (**Pt(II)porphyrin**) and four acenaphthene chromophores (**ANP**). In an air-equilibrated solution, energy transfer to O_2 quenches the porphyrin phosphorescence at 660 nm. Radiative processes are represented by solid lines and non-radiative processes by dashed lines. [52b]

In air-equilibrated solution **PtTANP** exhibits a very weak phosphorescence (Φ_{em} = 0.22%) with a much shorter lifetime (τ = 910 ns). The **PtTANP** phosphorescence is strongly quenched by oxygen with a rate constant of 4.9×10^8 $M^{-1}s^{-1}$, resulting in singlet oxygen production with a very high quantum yield of 88% (Figure S7). [53] The emission spectrum of **PtTANP** in a rigid matrix of DCM-MeOH 1:1 at 77K shows an intense phosphorescence with a small blue shift, compared to the phosphorescence at room temperature in dichloromethane (blue line in Figure 3). The emission lifetime is 91 µs, a higher value compared to 298 K thanks to the suppression of quenching and decrease of the rate of non-radiative decay processes at low temperatures.

Table 1 Most relevant photophysical data of the **PtTANP** and the other discussed Pt-porphyrin derivatives.

Compound	Absorption data		Emission data							Ref.
	298 K		298 K					77K		
	λ_{max} / nm	$\varepsilon/10^4$ $M^{-1}cm^{-1}$	λ_{ph} / nm	Φ_{ph}	τ / μs	$k_{ph}/10^3$ s^{-1}	$k'_{isc}/10^3$ s^{-1}	λ_{ph}/nm	τ / μs	
PtTANP	410, 512, 542	22.4, 3.0, 0.9	663	0.22% (35%)[g]	0.91 (75)[g]	4.67	0.87	653	91	this work[h]
PtTPP[a]	402, 510, 538	22.2, 1.6, 0.4	657	– (4.6%)[g]	– (57)[g]	0.81	16.7	655	132	54a, 32
PtTFP[b]	409, 512, 540 (sh)	31.6, 2.8, 0.45	679, 741	– (2%)[g]	– (22)[g]	0.91	44.5	661 730	102	32
PtTOFP[c]	267, 406, 511	–	683, 743	– (11%)[g]	– (48)[g]	2.29	18.5	669 741	105	54b
PtOOFP[d]	267, 406, 511, 541, 599	–	664, 729	– (4.2%)[g]	– (54)[g]	0.78	17.7	652 722	123	54b
PtTTEP[e]	404 512, 542	27.5, 2.7, 0.8	665, 731	– (5.1%)[g]	– (73)[g]	0.70	13.0	–	–	55
PtOEP[f]	381, 501, 536	–	644	–	– (50±20)[g]	–	–	–	121	55

[a]TPP = 5,10,15,20-tetraphenylporphyrin, [b]TFP= 5,10,15,20-meso-tetrakis(fluoren-2-yl)porphyrin,

[c] TOFP = 5,10,15,20-tetra(4-(2 methyloxyfluorenyl)phenyl)porphyrin, [d] OOFP = 5,10,15,20-octa(3,5-(2 methyloxyfluorenyl)phenyl)porphyrin,

[e] TTEP = 5,10,15,20-tetrakis[2,4,6-triethylphenyl]porphyrin, [f] OEP= octaethylporphyrin.

[g]Data in parenthesis refer to deaerated solutions. [h] in air-equilibrated dichloromethane solution.

We can now compare the photophysical properties of **PtTANP** with that of the parent compound 5,10,15,20-tetraphenylporphyrin Pt(II) complex, **PtTPP** [32, 53-55] (Table 1): the energy of the Soret band and Q-bands of **PtTANP** is similar with only a very modest red shift. A similar behavior has been reported previously upon the introduction of fluorenyl units (**PtTFP**)[32] and it has been attributed to the so-called in-plane nuclear reorganization. The manifestation of the in-plane nuclear reorganization could be realized while the more conjugated *meso* substituent draws the *meso* carbon away from the porphyrin core. While analysing the crystal data of **PtTPP** and **PtTANP**, we have observed that the distances of *meso*-carbon from the platinum center are ~3.42 Å for **PtTPP**. [50] While the similar distances in **PtTANP** are ~3.44 Å. We have considered the position of Pt^{2+} is at the center of the porphyrin core. This observation indicates that as the acenaphthyl is more conjugated than the phenyl ring thus it draws the *meso*-carbon away from the porphyrin core.

Assuming a unitary efficiency of the $S_1 \rightarrow T_1$ inter system crossing process (η_{isc}),[32] as expected by the presence of a the Pt heavy-atom, we can estimate the radiative (k_{ph}) and non-radiative (k'_{isc}) decay processes of the phosphorescent T_1 state by the measured values of phosphorescence quantum yield (Φ_{ph}) and lifetime of the T_1 excited state ($\tau(T_1)$) under deaerated conditions, according to the following equations:

$$\Phi_{ph} = \eta_{isc} \frac{k_{ph}}{k_{ph} + k'_{isc}}$$

$$\tau(T_1) = \frac{1}{k_{ph} + k'_{isc}}$$

The corresponding values are reported in Table 1.

The introduction of the acenaphthyl units brings about an increase in the radiative rate constant (k_{ph}) and a decrease of the non-radiative rate constant (k'_{isc}), compared to **PtTPP**. Both of these changes contribute to enhance the phosphorescence quantum yield. On the contrary, the previously reported fluorenyl substituent (**PtTFP**) causes an increase of both the radiative and non-radiative rate constants, thus decreasing the overall phosphorescence quantum yield. While comparing the photophysical properties of **PtTANP** with that of the other literature reported platinum porphyrin derivatives (Table 1), it is evident that the values of lifetime of the phosphorescent excited state and of the phosphorescence quantum yield in deaerated solutions at 298 K are the highest in the case of **PtTANP**. Furthermore, the phosphorescence quantum yield of **PtTANP** is strongly quenched by dioxygen. Indeed, **PtTANP** shows a very high singlet oxygen quantum yield of 88% in dichloromethane indicating that it is an excellent

photosensitiser for the production of singlet oxygen and potential application in the field of photodynamic therapy as well as oxygen sensors. [56,57]

Conclusions

In conclusion, we have synthesized a new platinum(II) porphyrin complex, [5,10,15,20-tetra(5-acenaphthyl)porphinato] platinum(II), **PtTANP** bearing acenaphthyl group at the *meso* position of the porphyrin ring. This complex has been thoroughly characterized via various spectroscopic techniques, including single-crystal XRD analysis. It was observed that the Pt(II) center in **PtTANP** is very near to the perfect square planar geometry. The Pt(II)-N bond distances are in the ranges of 2.005 Å─2.020 Å. The **PtTANP** derivative exhibited one reversible oxidative couple at +1.10 V and a reversible reductive couple at -1.47 V versus Ag/AgCl. In deaerated solution, a strong red phosphorescence is observed with emission quantum yield as high as 35% and emission lifetime of 75 μs. **PtTANP** works as a light-harvesting antenna: upon UV excitation of acenaphthene chromophores energy transfer to the Pt(II) porphyrin core takes place with unitary efficiency and results in the photosensitised phosphorescence. It was also demonstrated that the **PtTANP** molecule is an excellent photosensitizer having singlet oxygen production quantum yield of 88% in dichloromethane. A close comparison of **PtTANP** with that of the previously reported platinum porphyrin derivatives demonstrates its superiority. The lifetime of the phosphorescent excited state of **PtTANP** in deaerated solutions at 298 K is longer and its phosphorescence quantum yield is also significantly higher than the other reported platinum porphyrin derivatives. These results indicate that the **PtTANP** molecule will have potential applications in the field of photodynamic therapy as well as oxygen sensors.

Experimental Section

Materials: The precursor's pyrrole, benzonitrile, DDQ (2,3-Dichloro-5,6-dicyano-1,4-benzoquinone), 5-acenaphthene carboxaldehyde, K_2PtCl_4 (Potassium tetrachloroplatinate(II)), and TEAP (Tetraethyl ammonium perchlorate) were purchased from Aldrich, USA. Other chemicals were of reagent grade. Hexane and dichloromethane were distilled from KOH and CaH_2, respectively. For spectroscopy and electrochemical studies, HPLC grade solvents were used. **H_2TANP** was prepared by following an earlier literature report. [58]

Physical Measurements:

Luminescence measurements at 77 K were performed in dichloromethane/methanol (1:1 v/v). UV–vis absorption spectra were recorded with a PerkinElmer l40 spectrophotometer using quartz cells with path length of 1.0 cm. Emission spectra were obtained with either a Perkin Elmer LS55 spectrofluorometer, equipped with a Hamamatsu R928 phototube, or an Edinburgh FLS920 spectrofluorometer equipped with a Ge-detector for emission in the NIR spectral region. Correction of the emission spectra for detector sensitivity in the 550-1000 nm spectral region was performed by a calibrated lamp. [52b] Excitation spectra in the visible range were acquired with the fluorimeter Perkin-Elmer LS55. Emission quantum yields were measured following the method of Demas and Crosby [59] (standards used: $[Ru(bpy)_3]^{2+}$ in air-equilibrated aqueous solution $\Phi = 0.0405$.[60] Quantum yield of oxygen production is calculated by comparison between the oxygen phosphorescence generated by the sample and by a standard (standard used: 1H-Phenalen-1-one in toluene, $\Phi_\Delta = 0.95$).[61] Photophysical characterization in the absence of oxygen was carried out on samples of dye solutions after degassing them by freeze–pump–thaw cycling ($P = 10^{-9}$ Bar; liquid nitrogen as cooling medium) in a custom-made quartz cuvette. Emission intensity decay measurements in the range 10 μs to 1 s were performed on a homemade time-resolved phosphorimeter. Lifetimes shorter than 10 μs were measured by the above-mentioned Edinburgh FLS920 spectrofluorimeter equipped with a TCC900 card for data acquisition in time-correlated single-photon counting experiments (0.5 ns time resolution) with 405 nm laser. The estimated experimental errors are: 2 nm on the absorption and emission band maximum, 5% on the molar absorption coefficient and luminescence lifetime, and 10% on the luminescence and photoisomerization quantum yields. The elemental analyses were carried out with a Perkin–Elmer 240C elemental analyzer. The NMR measurements were carried out using a Bruker AVANCE 400 NMR spectrometer. Tetramethylsilane (TMS) was the internal standard. Electrospray mass spectra were recorded on a Bruker Micro TOF─QII mass spectrometer. Cyclic voltammetry measurements were

carried out using a CH Instruments model CHI1120A electrochemistry system. A glassy–carbon working electrode, a platinum wire as an auxiliary electrode, and a saturated calomel reference electrode (SCE) were used in a three–electrode configuration. Tetraethyl ammonium perchlorate (TEAP) was the supporting electrolyte (0.1M), and the concentration of the solution was 10^{-3}M with respect to the complex. The oxidation and reduction processes at the positive and negative sides of the Ag-AgCl reference electrode were measured by using a glassy–carbon working electrode. The half-wave potential E^0_{298} was set equal to 0.5(E_{pa} + E_{pc}), where E_{pa} and E_{pc} are anodic and cathodic cyclic voltammetric peak potentials, respectively. The scan rate used was 100 mV s^{-1}.

Crystal Structure Determination: Single crystals of [5,10,15,20-tetra(5-acenaphthyl)porphinato] platinum(II), **PtTANP** were grown by slow diffusion of a solution of the metal complexes in diethyl ether into dichloromethane, followed by slow evaporation under atmospheric conditions. The crystal data of **PtTANP** was collected on a Bruker Kappa APEX II CCD diffractometer at 293 K. Selected data collection parameters and other crystallographic results are summarized in Table S1. All data were corrected for Lorentz polarization and absorption effects. The program package SHELXTL [62] was used for structure solution and full matrix least-squares refinement on F^2. Hydrogen atoms were included in the refinement using the riding model. Contributions of H atoms for the water molecules were included but were not fixed. Disordered solvent molecules were taken out using SQUEEZE command in PLATON. [63] CCDC- 2075384 contains the supplementary crystallographic data for **PtTANP**. These data can be obtained free of charge via www.ccdc.cam.ac.uk/data_ request/cif.

Synthesis of [5,10,15,20-tetra(5-acenaphthyl)porphinato] platinum(II), PtTANP: **PtTANP** was prepared by slight modifications of an earlier reported protocols.[64] In a 100ml R.B. flask, 40 ml of benzonitrile was taken in a dry, degassed atmosphere. K_2PtCl_4 (167 mg, 0.4 mmol) was added to this benzonitrile (40ml) solvent, and the mixture was heated with stirring under an N_2 atmosphere at 100^0C. After 15 minutes, the solution turned out to be yellow. Then the 5,10,15,20-tetra(5-acenaphthyl) porphyrin, **H_2TANP** (50 mg, 0.05mmol) was added, and the resulting mixture was heated with stirring at reflux temperature for 48 hr. The mixture was cooled to room temperature, and the benzonitrile was removed by using rotary evaporation. Then the dried mass was subjected to column chromatography (Silica gel, dichloromethane /hexane eluent). The purest fractions were combined and dried by using rotary evaporation and crystallized as orange plates.

For [5,10,15,20-tetra(5-acenaphthyl)porphinato] platinum(II), PtTANP: Yield 38 mg (62 %); Anal. Calcd (found) for $C_{68}H_{44}N_4Pt$ (**PtTANP**): C, 73.43 (73.51); H, 3.99 (3.84); N, 5.04 (5.17). UV-Vis (dichloromethane): λ_{max}/nm ($\varepsilon/M^{-1}cm^{-1}$): 410 (224000), 512 (30000), 542 (9000). ^{1}H NMR (400 MHz, chloroform-*d*) δ 3.62-3.70 (m, 16 H), 6.81 - 7.02 (m, 4 H), 7.12 - 7.20 (m, 4 H), 7.29 - 7.30 (d, *J*=6.9 Hz, 4 H), 7.66 - 7.68 (d, *J*=7.6 Hz, 4 H), 8.08 - 8.18 (m, 4 H), 8.46 - 8.50 (m, 8 H) (Figure S1). ^{13}C NMR (101 MHz, $CDCl_3$) δ 151.25, 146.68, 145.72, 141.64, 138.72, 134.80, 134.26, 132.92, 132.32, 131.80, 130.88, 129.26, 128.38, 123.04, 121.86, 119.36, 118.16, 114.99, 112.60, 30.83, 30.57 (Figure S2). The electrospray mass spectrum in acetonitrile (Figure S3) showed the peaks centered at *m/z* = 1112.3391 corresponding to [**PtTANP**+H]$^+$(calculated molecular mass: 1112.3292). **PtTANP** displayed strong phosphorescence at 663 nm and 725 nm (Table 1).

Supporting information

Synthesis and characterization of **PtTANP**. ^{1}H NMR, ^{13}C NMR, ESI-MS spectrum and crystallographic data of **PtTANP**. CCDC 2075384 contains the supplementary crystallographic data for **PtTANP**. These data can be obtained free of charge via www.ccdc.cam.ac.uk/data_ request/cif.

Acknowledgments

Financial support received from the Department of Atomic Energy (India) is gratefully acknowledged. The authors thankfully acknowledge NISER-Bhubaneswar for providing infrastructure. The authors gratefully acknowledge the financial support provided by SERB (Science & Engineering Research Board), India (EMR/2016/005484), to carry out this research work. PC, MM and MV acknowledge the University of Bologna for the financial support.

KEYWORDS: Platinum / Porphyrinoids / Electrochemistry / Photochemistry / Singlet oxygen

Notes and references

[1] Y. You, W. Nam, *Chem. Soc. Rev.* **2012**, *41*, 7061-7084.

[2] J. Zhao, W. Wu, J. Sun, S. Guo, *Chem. Soc. Rev.* **2013**, *42*, 5323-5351.

[3] K. Kalyanasundaram, M. Grätzel, *Coord. Chem. Rev.* **1998**, *177*, 347-414.

[4] P. S. Wagenknecht, P. C. Ford, *Coord. Chem. Rev.* **2011**, *255*, 591-616.

[5] V. Balzani, P. Ceroni, A. Juris, M. Venturi, S. Campagna, F. Puntoriero, S. Serroni, *Coord. Chem. Rev.* **2001**, *219*, 545-572.

[6] V. Balzani, G. Bergamini, F. Marchioni, P. Ceroni, *Coord. Chem. Rev.* **2006**, *250*, 1254-1266.

[7] O. S. Wenger, *Coord. Chem. Rev.* **2009**, *253*, 1439-1457.

[8] N. A. Ludin, A. A.-A. Mahmoud, A. B. Mohamad, A. A. H. Kadhum, K. Sopian, N. S. A. Karim, *Renew. Sustain. Energy Rev.* **2014**, *31*, 386-396.

[9] A. Carella, F. Borbone, R. Centore, *Front. Chem.* **2018**, *6*, 481.

[10] M. Parasram, V. Gevorgyan, *Chem. Soc. Rev.* **2017**, *46*, 6227-6240.

[11] D. M. Guldi, M. Maggini, E. Menna, G. Scorrano, P. Ceroni, M. Marcaccio, F. Paolucci, S. Roffia, *Chem. Eur. J.* **2001**,*7*, 1597-1605.

[12] V. Balzani, G. Bergamini, P. Ceroni, *Rendiconti Lincei* **2017,** *28*, 125-142.

[13] M. C. DeRosa, R. J. Crutchley, *Coord. Chem. Rev.* **2002**, *233*, 351-371.

[14] N. Adarsh, R.R. Avirah, D. Ramaiah, *Org. Lett.* **2010**, *12*, 5720-5723.

[15] S. Mostafa, F.L. Rosario-Ortiz, *Environ. Sci. Technol.* **2013**, *47*, 8179-8186.

[16] Y. Qin, L. J. Chen, F. Dong, S.T. Jiang, G.Q. Yin, X. Li, Y. Tian, H.B. Yang, *J. Am. Chem. Soc.* **2019**, *141*, 8943–8950.

[17] A. Galstyan, Y. K. Maurya, H. Zhylitskaya, Y.J. Bae, Y.L. Wu, M.R. Wasielewski, T Lis, U. Dobrindt, M. Stępień, *Chem. Eur. J.* **2020**, *26*, 8262-8266.

[18] P Pushpanandan, D.H. Won, S. Mori, Y. Yasutake, S. Fukatsu, M. Ishida, H. Furuta, *Chem. Asian J.* **2019**, *14*, 1729-1736.

[19] S. Callaghan, M.O. Senge, *Photochem. Photobiol. Sci.* **2018**, *17*, 1490-1514.

[20] F. Heinemann, J. Karges, G. Gasser, *Acc. Chem. Res.* **2017**, *50*, 2727-2736.

[21] H. Huang, S. Banerjee, P.J. Sadler, *ChemBioChem* **2018**, *19*, 1574-1589.

[22] W. Sinha, L. Ravotto, P. Ceroni, S. Kar, *Dalton Trans.* **2015**, *44*, 17767-17773.

[23] L. Huang, M. Rudolph, F. Rominger, A. S. K. Hashmi, *Angew. Chem. Int. Ed.* **2016**, *55*, 4808-4813.

[24] M. Yang, J. Deng, D. Guo, J. Zhang, L. Yang, F. Wu, *Org. Biomol. Chem.* **2019**, *17*, 5367-5374.

[25] G.K. Couto, B.S. Pacheco, V.M. Borba, J.C.R. Junior, T.L. Oliveira, N.V. Segatto, F.K. Seixas, T.V. Acunha, B.A. Iglesias, T. Collares, *J. Photochem. Photobiol. B* **2020**, *202*, 111725.

[26] P. Lang, J. Habermehl, S.I. Troyanov, S. Rau, M. Schwalbe, *Chem. Eur. J.* **2018**, *24*, 3225-3233.

[27] H.C. Chen, D.G. Hetterscheid, R.M. Williams, J.I. van der Vlugt, J.N. Reek, A.M. Brouwer, *Energy Environ. Sci.* **2015**, *8*, 975-982.

[28] C. Lottner, K.C. Bart, G. Bernhardt, H. Brunner, *J. Med. Chem.* **2002**, *45*, 2064-2078.

[29] R.C. Kwong, S. Sibley, T. Dubovoy, M. Baldo, S.R. Forrest, M.E. Thompson, *Chem. Mater.* **1999**, *11*, 3709-3713.

[30] J. R. Sommer, A.H. Shelton, A. Parthasarathy, I. Ghiviriga, J.R. Reynolds, K.S. Schanze, *Chem. Mater.* **2011**, *23*, 5296-5304.

[31] I. Toubia, C. Nguyen, S. Diring, L.M. Ali, L. Larue, R. Aoun, C. Frochot, M. Gary-Bobo, M. Kobeissi, F. Odobel, *Inorg. Chem.* **2019**, *58*, 12395-12406.

[32] S. Drouet, C.O. Paul-Roth, V. Fattori, M. Cocchi, J.G. Williams, *New J. Chem.* **2011**, *35*, 438-444.

[33] A.-K. Bansal, W. Holzer, A. Penzkofer, T. Tsuboi, *Chem. Phys.* **2006**, *330*, 118-129.

[34] O. S. Finikova, A. Y. Lebedev, A. Aprelev, T. Troxler, F. Gao, C. Garnacho, S. Muro, R. M. Hochstrasser, S. A. Vinogradov, *ChemPhysChem* **2008**, *9*, 1673-1679.

[35] T. V. Esipova, H. c. J. Rivera-Jacquez, B. Weber, A. m. E. Masunov, S. A. Vinogradov, *J. Am. Chem. Soc.* **2016**, *138*, 15648-15662.

[36] J. N. Demas, B. A. DeGraff, P. B. Coleman, *Anal. Chem.* **1999**, *71*, 793A-800A.

[37] S. Ji, W. Wu, W. Wu, P. Song, K. Han, Z. Wang, S. Liu, H. Guo, J. Zhao, *J. Mater. Chem.* **2010**, *20*, 1953-1963.

[38] W.W.S. Lee, K.Y. Wong, X.M. Li, *Anal. Chem.* **1993**, *65*, 255-258.

[39] S.W. Lai, Y.J. Hou, C.M. H.L. Che, K.Y. Wong, C.K. Chang, N. Zhu, *Inorg. Chem.* **2004**, *43*, 3724-3732.

[40] V.D. Rumyantseva, N.P. Ivanovskaya, L.I. Konovalenko, S.V. Tsukanov, A.F. Mironov, N.S. Osin, *Russ. J. Bioorganic Chem.* **2008**, *34*, 239-244.

[41] R.R. de Haas, R.P. van Gijlswijk, E.B. van der Tol, H.J. Zijlmans, T. Bakker–Schut, J. Bonnet, N.P. Verwoerd, H.J. Tanke, *J. Histochem. Cytochem*. **1997**, *45*, 1279-1292.

[42] J. Kalinowski, W. Stampor, J. Szmytkowski, M. Cocchi, D. Virgili, V. Fattori, P. Di Marco, *J. Chem. Phys.* **2005**, *122*, 154710.

[43] A.N. Filippin, J.R. Sanchez-Valencia, J. Idígoras, M. Macias-Montero, M. Alcaire, F.J. Aparicio, J.P. Espinos, C. Lopez-Santos, F. Frutos, A. Barranco, J.A. Anta, *Adv. Mater. Interfaces* **2017**, *4*, 1601233.

[44] Y. Amao, K. Asai, T. Miyashita, I. Okura, *Polym. Adv. Technol.* **2000**, *11*, 705-709.

[45] M.M. Alam, F. Bolze, C. Daniel, L. Flamigni, C. Gourlaouen, V. Heitz, S. Jenni, J. Schmitt, A. Sour, B. Ventura, *Phys. Chem. Chem. Phys.* **2016**, *18*, 21954-21965.

[46] K.R. Graham, Y. Yang, J.R. Sommer, A.H. Shelton, K.S. Schanze, J. Xue, J.R. Reynolds, *Chem. Mater.* **2011**, *23*, 5305-5312.

[47] K. M. Kadish, K. M. Smith, R. Guilard, The Porphyrin Handbook, Vols. 1–20, Academic Press, San Diego, **2000–2003**.

[48] C. Jellimann, M. Mathé-Allainmat, J. Andrieux, S. Kloubert, J.A. Boutin, J.P. Nicolas, C. Bennejean, P. Delagrange, M. Langlois, *J. Med. Chem.* **2000**, *43*, 4051-4062.

[49] A. Garai, M. Kumar, W. Sinha, S. Chatterjee, C.S. Purohit, T. Som, S. Kar, *RSC Adv.* **2014**, *4*, 64119-64127.

[50] A.C. Hazell, *Acta Crystallogr. Sec.C: Crystal Structure Communications* **1984**, *40*, 751-753.

[51] P. Chen, O.S. Finikova, Z. Ou, S.A. Vinogradov, K.M. Kadish, *Inorg. Chem.* **2012**, *51*, 6200-6210.

[52] a) E. L. Elliott, A. Orita, D. Hasegawa, P. Gantzel, J. Otera, J. S. Siegel, *Org. Biomol. Chem.* **2005**, *3*, 581-583; b) M. Montalti, A. Credi, L. Prodi, T. M. Gandolfi, *Handbook of Photochemistry*, 3rd ed., Taylor & Francis, Boca Raton, **2006**.

[53] C.M. Che, Y.J. Hou, M.C. Chan, J. Guo, Y. Liu, Y. Wang, *J. Mater. Chem.* **2003**, *13*, 1362-1366.

[54] a) W. Wu, W. Wu, S. Ji, H. Guo, X. Wang, J. Zhao, *Dyes Pigm.* **2011**, *89*, 199-211; b) C.O. Paul-Roth, S. Drouet, A. Merhi, J.G. Williams, L.F. Gildea, C. Pearson, M.C. Petty, *Tetrahedron* **2013**, *69*, 9625-9632.

[55] A.G. Moiseev, E.A. Margulies, J.A. Schneider, F. Bélanger-Gariépy, D.F. Perepichka, *Dalton Trans.* **2014**, *43*, 2676-2683.

[56] a) S. Mathai, T.A. Smith, K.P. Ghiggino, *Photochem. Photobiol. Sci.* **2007**, *6*, 995-1002; b) N. Molupe, B. Babu, E. Prinsloo, A.Y. Kaassis, K. Edkins, J. Mack, T. Nyokong, *J Porphyr Phthalocyanines.* **2019**, *23*, 1486-1494.

[57] XD Wang, OS. Wolfbeis, *Chem. Soc. Rev.* **2014**, *43*, 3666-761.

[58] Z. I. Zhilina, S. V. Vodzinskii, S. A. Andronati, *Ukr. Khim. Zh. (Russ. Ed.)* **1990**, *56*, 1084-1088.

[59] G. A. Crosby, J. N. Demas, *J. Phys. Chem.* **1971**, *75*, 991-1024.

[60] K. Suzuki, A. Kobayashi, S. Kaneko, K. Takehira, T. Yoshihara, H. Ishida, Y. Shiina, S. Oishi, S. Tobita, *Phys. Chem. Chem. Phys.* **2009**, *11*, 9850–9860

[61] F. Prat, C. Martí, S. Nonell, X. Zhang, C. S. Foote, R. G. Moreno, J. L. Bourdelande, J. Font, *Phys. Chem. Chem. Phys.* **2001**, *3*, 1638-1643.

[62] G. M. Sheldrick, *Acta Crystallogr., Sect. A: Found. Crystallogr.* **2008**, *64*, 112-122.

[63] d. S. P. Van, A. L. Spek, *Acta Crystallogr., Sect. A: Found. Crystallogr.* **1990**, *A46*, 194-201.

[64] L. M. Mink, M. L. Neitzel, L. M. Bellomy, R. E. Falvo, R. K. Boggess, B. T. Trainum, P. Yeaman, *Polyhedron* **1997**, *16*, 2809.